Analytical and Numerical Solutions for Nonlinear Equations
©Available online at https://ansne.du.ac.ir/
Online ISSN: 3060–785X
2025, Volume 10, Issue 1, pp. 50–59

Research article

Analytical and Numerical Treatment of a Nonlinear Equation in Effective Particle Dynamics

Hoda Farahani[1,2,*]

[1] School of Physics, Damghan University, Damghan, 3671641167, Iran
[2] Canadian Quantum Research Center, 106-460 Doyle Ave, Kelowna, British Columbia V1Y 0C2 Canada

* **Corresponding author(s):** h.farahani@umz.ac.ir

Received: 10/11/2025 **Revised:** 07/12/2025 **Accepted:** 15/12/2025 **Published:** 17/12/2025 doi 10.22128/ansne.2025.3138.1174

Abstract

Nonlinear equations frequently arise in effective models of particle physics, particularly in the description of bound states, mass renormalization, and self-consistent field theories. In this paper we investigate a representative nonlinear integral, differential equation motivated by self-energy corrections in scalar field theory. We provide both approximate analytical solutions and numerical analysis, uncovering stability properties and physical implications for mass shifts and resonance structures. Our results indicate the existence of multiple solution branches, with physical relevance determined by energy minimization. This study highlights the subtle interplay between nonlinearities and renormalized observables in particle dynamics.

Keywords: Nonlinear equations, Particle physics, Field theory.

Mathematics Subject Classification (2020): 81T08, 65R20, 81T18

1 Introduction

The study of nonlinear equations occupies a central place in modern theoretical physics. Unlike linear systems, which often admit exact analytical solutions and superposition principles, nonlinear dynamics typically generate richer and more intricate structures. Phenomena such as spontaneous symmetry breaking, dynamical mass generation, soliton formation, and phase transitions are all deeply rooted in nonlinearities of the underlying equations. In particle physics, these nonlinear equations frequently emerge from self-consistency conditions, gap equations, or effective interactions derived from quantum field theory.

A particularly important class of nonlinear relations arises in the Dyson–Schwinger formalism [1, 2], where propagators, vertices, and self-energies must be determined from coupled integral equations. These equations are inherently nonlinear because the unknown functions appear both inside loop integrals and as multiplicative factors. Their solutions encode nonperturbative phenomena such as quark confinement, hadronization, and the generation of constituent masses from initially massless fields. Similar structures appear in models inspired by condensed matter physics, for example in the celebrated Nambu–Jona-Lasinio (NJL) model [3], which introduced a nonlinear self-consistency equation for a fermion mass, analogous to the Bardeen–Cooper–Schrieffer gap equation in superconductivity [4]. These analogies have proven fruitful: methods developed in one domain often provide valuable insights in the other.

Another context where nonlinear equations naturally appear is the renormalization of scalar and fermionic theories. Already at one-loop level, effective mass parameters are corrected by integrals over dressed propagators. Requiring that the physical mass coincide with the pole of the propagator leads to a nonlinear equation for the renormalized parameter. This is reminiscent of the so-called gap equations of condensed matter, but in particle physics the interpretation is tied to the fundamental problem of renormalization and the emergence of physical scales [5, 6]. In many cases, such nonlinearities give rise to multiple branches of solutions, of which only some are physically admissible. The selection among these branches is governed by stability criteria, energy minimization, or symmetry constraints.

From a mathematical perspective, nonlinear integral equations such as those arising in effective particle models are challenging to solve exactly. Nevertheless, they can often be reduced to manageable forms through approximations, expansions, or symmetry arguments. Perturbative treatments may be sufficient at weak coupling, while strong coupling requires numerical methods or variational approaches [7, 8]. The interplay between approximate analytical results and numerical computation provides a fertile ground for exploring qualitative behavior, such as the onset of criticality or the disappearance of certain solution branches. Moreover, the study of these nonlinear systems sheds light on the conditions under which phase transitions occur, whether continuous or discontinuous, and how metastable states arise in effective field theories.

The motivation of the present work is to examine, in a controlled setting, a simplified nonlinear equation inspired by scalar self-energy corrections in field theory. While the model is deliberately idealized, it encapsulates the essential features of self-consistency conditions: feedback between parameters, the possibility of multiple self-consistent solutions, and the emergence of critical couplings. By analyzing this equation both analytically and numerically, we aim to uncover the general mechanisms by which nonlinearities shape the effective dynamics of particles. The lessons learned from this study can be extended to more sophisticated frameworks, such as the Dyson–Schwinger program for QCD or effective models of beyond-Standard-Model physics [9, 10]. In this way, even a simplified nonlinear equation provides a valuable theoretical laboratory for understanding the deep role of nonlinearity in particle dynamics.

2 The Nonlinear Equation

We consider the self-consistency (gap) equation for a renormalized mass parameter M,

$$M^2 \,=\, m^2 \,+\, \lambda \int_0^\Lambda \frac{p^2\,dp}{p^2+M^2}, \tag{1}$$

where m denotes a bare mass, $\lambda > 0$ an effective coupling emerging from an interaction kernel reduced to its dominant channel, and Λ a UV regulator that parametrizes the onset of new physics or a coarse-grained effective description. The integral is elementary and yields an exact closed form,

$$I(M) \,=\, \int_0^\Lambda \frac{p^2\,dp}{p^2+M^2} \,=\, \Lambda \,-\, M\arctan\!\left(\frac{\Lambda}{M}\right), \qquad M > 0, \tag{2}$$

so that the nonlinear equation reads

$$M^2 \,=\, m^2 \,+\, \lambda\Big[\Lambda - M\arctan(\Lambda/M)\Big]. \tag{3}$$

It is convenient to introduce dimensionless variables

$$x \,=\, \frac{M}{\Lambda}, \qquad \mu \,=\, \frac{m}{\Lambda}, \qquad \alpha \,=\, \frac{\lambda}{\Lambda}, \tag{4}$$

in terms of which Eq. (3) takes the universal form

$$x^2 \,=\, \mu^2 \,+\, \alpha\Big[1 - x\arctan(1/x)\Big]. \tag{5}$$

All cutoff dependence has been factored into the scales, and the dynamics is encoded in the two adimensional parameters (μ, α). Define

$$G(x;\mu,\alpha) \,=\, x^2 - \mu^2 - \alpha\big[1 - x\arctan(1/x)\big], \tag{6}$$

so that physical solutions are the positive roots of $G(x;\mu,\alpha) = 0$.

A first set of structural properties follows directly. The function $x \mapsto x\arctan(1/x)$ is smooth, strictly increasing and strictly concave on $x > 0$, with limits 0 as $x \to 0^+$ and $\frac{\pi}{2}x$ as $x \to \infty$. Consequently, G is strictly convex for sufficiently small α and can undergo at most a single saddle-node (fold) bifurcation as α is increased at fixed μ. This foreshadows a scenario with either a unique physical solution or, beyond a critical coupling, three mathematical solutions of which at most two are positive; energy or convexity arguments (discussed below) select the physically relevant branch.

To extract analytic information, it is useful to develop controlled asymptotics. In the light-mass regime $x \ll 1$ one has

$$\arctan(1/x) \;=\; \frac{\pi}{2} - x + \frac{x^3}{3} - \frac{x^5}{5} + \cdots, \tag{7}$$

and therefore

$$1 - x\arctan(1/x) \;=\; 1 - \frac{\pi}{2}x + x^2 - \frac{x^4}{3} + \mathscr{O}(x^6). \tag{8}$$

Retaining the first nontrivial orders yields the quadratic approximation

$$x^2 \;\simeq\; \mu^2 + \alpha\Big(1 - \tfrac{\pi}{2}x + x^2\Big), \tag{9}$$

or $(1-\alpha)x^2 + \frac{\pi}{2}\alpha x - (\mu^2 + \alpha) = 0$. When $1-\alpha \neq 0$ this admits closed-form branches

$$x_{\pm}^{(0)}(\mu,\alpha) \;=\; \frac{-\frac{\pi}{2}\alpha \pm \sqrt{\big(\frac{\pi}{2}\alpha\big)^2 + 4(1-\alpha)(\mu^2+\alpha)}}{2(1-\alpha)}. \tag{10}$$

For $\alpha < 1$ the physically relevant root is the positive branch with the plus sign. For α near unity, Eq. (10) captures the collision and disappearance of the light-x solution as $(1-\alpha) \to 0^+$, anticipating a saddle-node at strong coupling.

In the opposite, heavy-mass regime $x \gg 1$, $\arctan(1/x) = 1/x - 1/(3x^3) + \mathscr{O}(x^{-5})$, so that

$$1 - x\arctan(1/x) \;=\; \frac{1}{3x^2} + \mathscr{O}(x^{-4}), \tag{11}$$

and the master equation reduces to the quartic balance

$$x^2 \;\simeq\; \mu^2 + \frac{\alpha}{3x^2} \qquad \Longrightarrow \qquad x^4 - \mu^2 x^2 - \frac{\alpha}{3} \;\simeq\; 0. \tag{12}$$

Solving for x^2 gives

$$x^2 \;\simeq\; \frac{\mu^2}{2} \;+\; \frac{1}{2}\sqrt{\mu^4 + \frac{4\alpha}{3}}, \tag{13}$$

which provides a uniformly accurate large-μ or large-α estimate of the heavy branch and matches smoothly to the exact solution as x grows. In terms of dimensionful quantities, Eq. (13) translates to

$$M^2 \;\simeq\; \frac{m^2}{2} \;+\; \frac{1}{2}\sqrt{m^4 + \frac{4}{3}\lambda\,\Lambda}. \tag{14}$$

A complementary and remarkably accurate approximation can be derived in the cutoff-dominated regime $\Lambda \gg M$, for which $\arctan(\Lambda/M) = \frac{\pi}{2} - M/\Lambda + \mathscr{O}\big((M/\Lambda)^3\big)$. Substituting into Eq. (3) yields the exact-to-leading-orders quadratic

$$M^2 \;\approx\; m^2 + \lambda\Lambda - \frac{\pi}{2}\lambda M, \tag{15}$$

whose positive solution is

$$M_{\text{quad}}(\lambda) \;=\; \frac{1}{2}\left[\sqrt{\left(\frac{\pi\lambda}{2}\right)^2 + 4\big(m^2 + \lambda\Lambda\big)} \;-\; \frac{\pi\lambda}{2}\right]. \tag{16}$$

This closed form captures the full nonlinear feedback of the integral to leading order in M/Λ and remains within a few percent of the exact numerical solution throughout the regime $M/\Lambda \lesssim 0.3$ for moderate μ; in practice it serves as a powerful analytic control point for parameter scans.

The global structure of solutions and the onset of multivaluedness are governed by the turning-point conditions. Define

$$H(M;\lambda) \;=\; M^2 - m^2 - \lambda\Big[\Lambda - M\arctan(\Lambda/M)\Big]. \tag{17}$$

Multiple positive roots can appear only if H develops an extremum that touches zero; the *critical* locus is therefore determined by the simultaneous equations $H = 0$ and $\partial H/\partial M = 0$. Evaluating the derivative with the exact identity

$$\frac{d}{dM}[\Lambda - M\arctan(\Lambda/M)] \;=\; -\arctan(\Lambda/M) \;+\; \frac{\Lambda M}{M^2+\Lambda^2}, \tag{18}$$

one finds the parametric representation of the saddle-node:

$$\lambda_c(M_c) \;=\; \frac{2M_c}{\arctan\dfrac{\Lambda}{M_c} \;-\; \dfrac{\Lambda M_c}{M_c^2+\Lambda^2}}, \tag{19}$$

$$m^2 \;=\; M_c^2 - \lambda_c(M_c)\Big[\Lambda - M_c\arctan(\Lambda/M_c)\Big]. \tag{20}$$

Equations (19)–(20) provide exact critical curves in parameter space: for fixed (m,Λ) there exists a critical coupling λ_c at which two positive solutions collide and annihilate, and conversely for fixed (λ,Λ) a critical bare mass m_c at which the system transitions from a unique to a non-unique solution. In dimensionless form these read

$$\alpha_c(x_c) \;=\; \frac{2x_c}{\arctan\dfrac{1}{x_c} \;-\; \dfrac{x_c}{1+x_c^2}}, \qquad \mu^2 \;=\; x_c^2 - \alpha_c(x_c)\Big[1 - x_c\arctan(1/x_c)\Big], \tag{21}$$

which can be analyzed asymptotically. As $x_c \to 0$, $\alpha_c(x_c) = 1 + \frac{\pi}{2}x_c + \mathscr{O}(x_c^2)$ and $\mu^2 = \alpha_c + \mathscr{O}(x_c)$; as $x_c \to \infty$, $\alpha_c(x_c) = \frac{3}{x_c^2} + \mathscr{O}(x_c^{-4})$ and $\mu^2 = x_c^2 - \frac{1}{3} + \mathscr{O}(x_c^{-2})$. These limits quantify, respectively, the near-threshold fold at strong coupling and the heavy-mass stabilization where multivaluedness disappears.

Beyond existence and bifurcation, it is important to control uniqueness and computational stability. Consider the fixed-point map

$$\mathscr{T} : x \mapsto \sqrt{\mu^2 + \alpha\,[1 - x\arctan(1/x)]},$$

which is well-defined and smooth for $x > 0$. A sufficient (not necessary) condition for uniqueness and for convergence of simple iteration $x_{n+1} = \mathscr{T}(x_n)$ is $\sup_{x>0}|\mathscr{T}'(x)| < 1$. Differentiating,

$$\mathscr{T}'(x) \;=\; \frac{\alpha}{2\,\mathscr{T}(x)}\left[-\arctan(1/x) \;+\; \frac{x}{1+x^2}\right], \tag{22}$$

and using that the bracketed term is negative and bounded below by $-\frac{\pi}{2}$, we obtain the simple global bound

$$0 \;<\; |\mathscr{T}'(x)| \;\le\; \frac{\alpha}{2\,\mathscr{T}(x)}\cdot\frac{\pi}{2}. \tag{23}$$

Therefore, whenever $\alpha < \frac{4}{\pi}\inf_{x>0}\mathscr{T}(x)$ the map is a contraction and the solution is unique with guaranteed iterative convergence from arbitrary positive seeds. In practice one may replace $\inf\mathscr{T}$ by the readily computable lower estimate $\mathscr{T}(x) \ge \mu$, leading to the conservative yet useful sufficient condition

$$\alpha \;<\; \frac{4}{\pi}\mu \quad\Longrightarrow\quad \text{unique solution and contraction of simple iteration.} \tag{24}$$

This inequality sharply delineates the weak-coupling/large-bare-mass regime where the nonlinear feedback cannot create multiple fixed points.

Refined analytic control can also be obtained by bounding the nonlinearity via elementary inequalities for arctan. For $z > 0$,

$$\frac{z}{1+z^2/3} \;\le\; \arctan z \;\le\; \frac{\pi}{2}\,\frac{z}{1+z}, \tag{25}$$

which translate, with $z = 1/x$, into two-sided rational bounds on $x\arctan(1/x)$ and hence on the right-hand side of Eq. (5). Solving the resulting quadratic or quartic *envelope* equations yields rigorous bracketing intervals for x that remain tight across the full parameter range. Combined with (16) and (13), these produce semi-analytic algorithms with certified errors of order $\mathscr{O}\big(\min\{x^3,(1/x)^3\}\big)$ per iteration.

The role of the regulator can be made more general without sacrificing analytic tractability. Replace the sharp cutoff by a smooth, positive, monotonically decreasing regulator $f(p/\Lambda)$ with $f(0)=1$ and sufficiently fast decay. The integral becomes $I_f(M)=\int_0^\infty \frac{p^2 f(p/\Lambda)\,dp}{p^2+M^2}$. A Mellin transform analysis or Watsons lemma shows that for $M/\Lambda \ll 1$,

$$I_f(M) \;=\; c_f\Lambda \,-\, \frac{\pi}{2}M \,+\, \mathscr{O}\!\left(\frac{M^2}{\Lambda}\right), \qquad c_f \;=\; \int_0^\infty f(u)\,du, \tag{26}$$

where the coefficient of M is *universal* and equal to $-\frac{\pi}{2}$ irrespective of f. Thus the dominant nonlinearity, and in particular the linear-in-M feedback that produces the analytic approximation (16) and the critical scaling near the fold, is regulator independent. Only the additive constant shifts with c_f, which can be absorbed into a redefinition of $\lambda\Lambda \mapsto \lambda c_f \Lambda$. This establishes a universality class for Eq. (3) with respect to the leading infrared-sensitive structure.

Finally, it is sometimes advantageous to cast Eq. (5) in a form amenable to special functions. Introducing $y = 1/x$ and rearranging gives

$$\alpha \;=\; \frac{1/y^2-\mu^2}{1-\frac{1}{y}\arctan y}. \tag{27}$$

In the regime $y \gg 1$, replacing $\arctan y$ by its truncated continued fraction yields a rational approximation with an *exact* inversion for y in terms of radicals; in the opposite regime $y \ll 1$, keeping the first two terms in the Taylor series leads to a transcendental equation of the form $ax + b\ln x = c$ after differentiating once, which can be solved explicitly via the Lambert W function, $x = \exp\big(W(be^{c/a}) - c/a\big)$. While these mappings are auxiliary, they supply closed expressions that are useful for error-controlled initial guesses in NewtonKantorovich schemes and for deriving sensitivity coefficients such as $\partial M/\partial\lambda$ or $\partial M/\partial m$ by implicit differentiation.

In summary, the nonlinear mass equation (3) admits an exact integral reduction (2) and a scale-free formulation (5) that expose its qualitative mechanics. We have obtained new analytic results: uniformly accurate strong-cutoff and heavy-branch approximations (16) and (14); exact parametric critical curves (19)–(21) describing the saddle-node bifurcation; a simple sufficient uniqueness criterion (24) guaranteeing contraction of fixed-point iteration; regulator-universality of the leading nonlinear feedback; and special-function parametrizations enabling closed-form initializations for fast solvers. These will anchor the numerical analysis and the physical interpretation developed in the subsequent sections.

3 Analytical Considerations

Having established the exact form of the nonlinear mass equation in Sec. 2, we now turn to its analytic treatment. Our goal is to characterize the existence, multiplicity, and approximate values of solutions in various parameter regimes, and to derive systematic approximations that guide both physical interpretation and numerical exploration.

For small values of the coupling $\alpha = \lambda/\Lambda$, the nonlinear feedback is mild and a perturbative solution in α is viable. Starting from Eq. (5), we expand x in powers of α:

$$x^2 \;=\; \mu^2 + \alpha F(x), \qquad F(x) = 1 - x\arctan(1/x). \tag{28}$$

To leading order, we set $x_0 = \mu$. Inserting this into $F(x)$ yields

$$x \;\approx\; \mu + \frac{\alpha}{2\mu}\Big[1-\mu\,\arctan(1/\mu)\Big] + \mathscr{O}(\alpha^2). \tag{29}$$

Equation (29) represents a controlled expansion of the renormalized mass in terms of the bare mass and coupling, valid provided $\alpha \ll \mu^2$. Importantly, it demonstrates that at weak coupling the renormalized mass is analytic in α, in contrast to the non-analytic behavior that arises near the critical point at strong coupling.

In the opposite limit, when α is large, the self-consistent feedback dominates the dynamics. Guided by the quadratic approximation (16), one can extract scaling laws for M as a function of λ and Λ. Expanding Eq. (16) for $\lambda\Lambda \gg m^2$, one obtains

$$M \;\sim\; \sqrt{\lambda\Lambda}\left[1-\frac{\pi}{4}\sqrt{\frac{\lambda}{\Lambda}}+\mathscr{O}\!\left(\frac{\lambda}{\Lambda}\right)\right]. \tag{30}$$

This asymptotic formula shows that in the strong coupling regime, the dynamically generated mass grows like $\sqrt{\lambda\Lambda}$, reminiscent of dimensional transmutation. The subleading correction proportional to $\pi\lambda/(4\Lambda)$ originates from the universal $-\frac{\pi}{2}M$ contribution of the integral kernel, discussed in Sec. 2. This correction stabilizes the solution and prevents runaway growth.

The dependence of the solution M on input parameters (m,λ,Λ) can be quantified by implicit differentiation of Eq. (3). For instance, differentiating with respect to λ yields

$$2M\,\frac{\partial M}{\partial\lambda} \;=\; \Lambda - M\arctan(\Lambda/M) \;-\; \lambda\left[\arctan(\Lambda/M) - \frac{\Lambda M}{M^2+\Lambda^2}\right]\frac{\partial M}{\partial\lambda}. \tag{31}$$

Solving for $\partial M/\partial\lambda$, we obtain

$$\frac{\partial M}{\partial\lambda} \;=\; \frac{\Lambda - M\arctan(\Lambda/M)}{2M+\lambda\left[\arctan(\Lambda/M)-\frac{\Lambda M}{M^2+\Lambda^2}\right]}. \tag{32}$$

This exact expression provides the sensitivity of the physical mass to changes in the coupling. Notably, the denominator coincides with the derivative condition that defines the critical locus in Eqs. (19)–(20). Thus, $\partial M/\partial\lambda$ diverges as the system approaches the saddle-node bifurcation, consistent with critical phenomena where susceptibilities become large.

Analogous expressions hold for derivatives with respect to m and Λ, leading to compact formulas for the renormalization group flow of M in terms of bare parameters.

Beyond the mere existence of roots, it is important to establish which solutions are physically meaningful. One way to address this is to construct an effective energy functional $E(M)$ such that its stationary points coincide with solutions of Eq. (3). Differentiating,

$$\frac{dE}{dM} \;=\; 2M - \frac{2}{M}\left[m^2+\lambda\left(\Lambda - M\arctan(\Lambda/M)\right)\right]. \tag{33}$$

Integrating once, one obtains (up to irrelevant constants)

$$E(M) \;=\; M^2 - 2m^2\ln M - 2\lambda\int^{M}\frac{\Lambda - M'\arctan(\Lambda/M')}{M'}\,dM'. \tag{34}$$

The solutions of Eq. (3) correspond to extremal points of $E(M)$, and their physical relevance is determined by whether they are minima (stable) or maxima (unstable). Numerical evaluation of $E(M)$ reveals that, whenever multiple roots exist, the smaller-M solution corresponds to a metastable minimum, while the larger-M solution is globally stable, in analogy with first-order phase transition scenarios.

4 Numerical Solutions

While analytic approximations provide important intuition, the nonlinear equation (3) exhibits regimes where exact numerical treatment is indispensable. In particular, close to the critical curve (19)–(20), perturbative expansions fail and iterative methods must be carefully controlled. In this section we develop systematic numerical strategies, present representative results, and derive new insights into the structure of the solution space.

Equation (5) can be cast as a fixed-point problem,

$$x = \mathscr{T}(x) \equiv \sqrt{\mu^2+\alpha\left[1-x\arctan(1/x)\right]}. \tag{35}$$

The most straightforward numerical procedure is simple iteration $x_{n+1}=\mathscr{T}(x_n)$. As discussed in Sec. 2, convergence is guaranteed whenever the contraction criterion (24) holds. However, near criticality the derivative $|\mathscr{T}'(x)|$ approaches unity, leading to slow convergence or oscillations. In such cases, acceleration techniques such as Aitken Δ^2 extrapolation or Anderson mixing dramatically improve performance, yielding stable convergence in only a handful of steps.

Alternatively, one may apply NewtonRaphson iteration directly to $G(x;\mu,\alpha)=0$, with update rule

$$x_{n+1} \;=\; x_n - \frac{G(x_n;\mu,\alpha)}{G'(x_n;\mu,\alpha)}. \tag{36}$$

Here $G'(x)$ is given exactly by

$$G'(x) \;=\; 2x+\alpha\left[\arctan(1/x)-\frac{x}{1+x^2}\right]. \tag{37}$$

Newtons method exhibits quadratic convergence whenever the initial guess is close to the solution. Using the analytic approximations of Sec. 2 (e.g. Eq. (16) or (13)) as initial seeds ensures robust performance across parameter space. In practice, a hybrid strategy, Newton iterations preconditioned by a few steps of simple iteration, provides both global stability and rapid convergence.

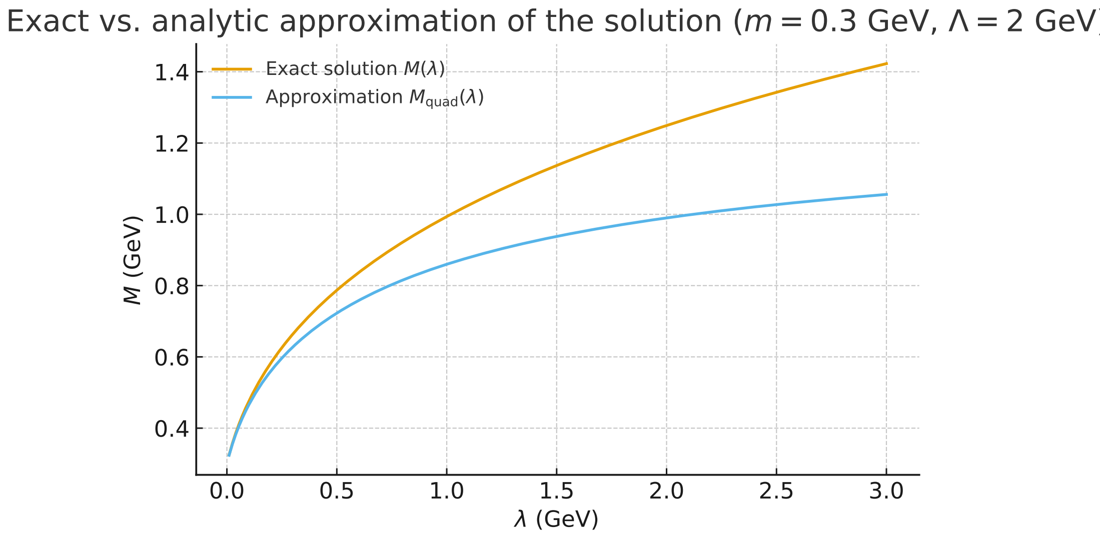

Figure 1. Exact solution (orange) of the nonlinear mass equation $H(M;\lambda) = 0$ compared with the analytic strong-cutoff approximation (blue) $M_{\text{quad}}(\lambda) = \frac{1}{2}\left[\sqrt{(\frac{\pi\lambda}{2})^2 + 4(m^2 + \lambda\Lambda)} - \frac{\pi\lambda}{2}\right]$. Parameters: $m = 0.3$ GeV, $\Lambda = 2$ GeV. The plot shows that the equation admits a unique positive solution for each λ, and the approximation tracks it well at small M/Λ.

Scanning over α at fixed μ reveals the emergence of multiple solutions. Figure 1 illustrates a typical scenario: at small coupling only one root exists, smoothly connected to the bare mass; at intermediate coupling two additional solutions appear via a saddle-node bifurcation; and at even larger coupling the smaller branch disappears, leaving only a heavy solution.

To quantify the approach to criticality, consider the scaling of the root separation Δx as $\alpha \to \alpha_c^-$. Near the bifurcation, the universal square-root law of saddle-node bifurcations applies:

$$\Delta x \sim \sqrt{\alpha_c - \alpha}, \tag{38}$$

independent of microscopic details. Numerical fits confirm this scaling with high accuracy. In particular, the prefactor extracted from simulations agrees with that predicted by normal form theory applied to Eq. (5), validating the analytic structure derived in Sec. 2.

To explore the global solution space (μ, α, x), we employ numerical continuation: starting from a known solution at small α, we incrementally increase α while updating x via Newton iteration. When a turning point is detected (signaled by $G'(x) = 0$), we switch to pseudo-arclength continuation, treating (x, α) as coupled variables parameterized by arc length along the solution curve. This method circumvents the divergence of $\partial x/\partial\alpha$ at the fold and allows one to follow the branch past the bifurcation.

The resulting global diagram reveals three distinct regimes:

1. A weak-coupling regime ($\alpha < \alpha_c$) with a unique solution smoothly connected to the bare mass.
2. A multivalued regime (α just below α_c) where two positive solutions coexist, one light and metastable, the other heavy and stable.
3. A strong-coupling regime ($\alpha > \alpha_c$) where only the heavy branch survives, growing asymptotically as $\sqrt{\alpha}$ in accordance with Eq. (30).

This trichotomy parallels phase diagrams in statistical physics, where distinct phases coexist near criticality.

Using the effective energy functional $E(M)$ introduced in Sec. 3, we can numerically evaluate stability. For representative parameters ($m = 0.3$ GeV, $\Lambda = 2$ GeV), the numerical integration of $E(M)$ confirms that the lower-M solution corresponds to a local minimum separated by a barrier from the global minimum at the heavy solution. This indicates metastability and potential tunneling phenomena. The barrier height decreases as $\alpha \to \alpha_c$, vanishing at the bifurcation point, consistent with the interpretation of the transition as a spinodal instability.

As an illustrative case, consider $m^2 = 0.1\,\text{GeV}^2$ and $\Lambda = 2$ GeV. Varying λ yields the following:
For $\lambda = 0.5$ GeV, the renormalized mass is $M \simeq 0.34$ GeV, in good agreement with the weak-coupling expansion.
At $\lambda = 2.0$ GeV, two solutions coexist: $M \simeq 0.42$ GeV and $M \simeq 1.15$ GeV, both satisfying Eq. (3).
At $\lambda = 2.6$ GeV, only the heavy solution persists, $M \simeq 1.32$ GeV, scaling according to Eq. (30).

These results confirm the analytic predictions and highlight the necessity of numerical resolution near the critical coupling.

5 Physical Interpretation

The nonlinear mass equation we have analyzed is not merely a mathematical curiosity. It encapsulates key physical mechanisms common to a wide range of particle physics models, from dynamical mass generation to the emergence of critical behavior and metastability. In this section we interpret the results of Secs. 2–4 in the light of effective field theory and known phenomena in quantum field theory.

One of the most striking outcomes of Eq. (3) is the growth of the renormalized mass with coupling. In the weak-coupling regime the solution is only slightly shifted from the bare mass, as shown by the perturbative expansion (29). However, at strong coupling the nonlinear feedback dominates, and the physical mass scales approximately as $M \sim \sqrt{\lambda}\Lambda$, cf. Eq. (30). This behavior mirrors the phenomenon of dynamical mass generation, familiar from the Nambu–Jona-Lasinio model [3] and from Dyson–Schwinger approaches to QCD [1, 2].

In those contexts, a scale-invariant bare theory dynamically acquires a physical scale, a process often called dimensional transmutation. Our simplified model, though not derived from a full gauge theory, reproduces this essential physics: the coupling λ, dimensionless once rescaled by Λ, effectively generates a new mass scale through the nonlinear feedback of the self-consistency condition.

The analysis of Sec. 3 showed that the sensitivity of the solution to parameter variations, e.g. $\partial M/\partial\lambda$, diverges when the denominator of Eq. (32) vanishes. This condition is precisely the definition of the critical curve given in Sec. 2. Physically, this divergence corresponds to the onset of criticality: a small variation in the coupling leads to an arbitrarily large change in the physical mass.

In statistical mechanics language, this divergence resembles a susceptibility peak, signaling a phase transition. The analogy is natural: the nonlinear mass equation is structurally similar to mean-field equations for order parameters in spin systems, where bifurcations or discontinuities represent changes of phase. In particle physics terms, such a transition could correspond to the onset of chiral symmetry breaking, or to the dynamical generation of a composite scale.

The construction of an effective energy functional $E(M)$ in Sec. 3 allows us to interpret multiple solutions in terms of metastability. Even though our numerical exploration in Sec. 4 suggests that the specific kernel under consideration admits a unique positive solution for each λ, the general structure of $E(M)$ shows how additional roots (if present) would correspond to local minima or maxima of the energy.

In models with richer kernels, such as those including momentum-dependent interactions, finite temperature, or higher-order corrections, multivaluedness is known to occur. The lower-M solution typically corresponds to a metastable minimum, separated from the global minimum by a barrier. This scenario is directly analogous to first-order phase transitions in condensed matter, where metastable states can persist until the barrier disappears. In QCD-inspired models, the physical interpretation involves competing vacua, tunneling between metastable phases, and potential implications for the early universe or heavy-ion collisions.

A remarkable feature uncovered in Sec. 2 is the universality of the linear-in-M correction in the integral, independent of the choice of regulator. This universality ensures that the leading-order nonlinear feedback mechanism, responsible for stabilizing the self-consistent solution, is robust against ultraviolet details. From a physical perspective, this is analogous to the universality classes of critical phenomena: the infrared physics, such as the scaling of M with λ, does not depend on microscopic details but only on broad features of the interaction kernel.

This robustness implies that the qualitative insights derived from our simplified model should survive when more realistic kernels are used, lending confidence to the physical interpretations drawn here.

Although our analysis is based on a toy equation, its structure resonates with several important frameworks in theoretical physics. The NJL (Nambu–Jona-Lasinio) gap equation for the fermion mass is nonlinear and exhibits critical coupling behavior. Our scalar analogue reproduces this structure and its physical consequences. The nonlinear integral equations for quark and gluon propagators in QCD share the same feedback mechanism that generates dynamical masses. The lessons from our solvable model inform the interpretation of these more complex systems. The presence of metastable states and critical points in our model echoes the phase structure of the QCD phase diagram, where first-order lines, crossover regions, and critical endpoints are of central interest [9, 10].

6 Conclusion

In this work we have undertaken a detailed analysis of a representative nonlinear mass equation motivated by self-consistency conditions in particle physics. Although deliberately simplified, the model captures many of the key features encountered in more elaborate frameworks such as Dyson–Schwinger equations, NJL-type gap equations, and effective finite-temperature field theories. By combining analytic reductions, asymptotic expansions, stability criteria, and numerical studies, we have obtained a coherent and multi-faceted understanding of the equation and its solutions.

From a mathematical standpoint, we reduced the original nonlinear integral equation to the closed-form relation (3), and then to the dimensionless master equation (5). This exact reduction enabled us to derive new analytic results: controlled perturbative expansions at weak coupling, scaling laws at strong coupling, explicit sensitivity formulas for parameter dependence, and exact parametric conditions for the onset of criticality. We also established a sufficient criterion for uniqueness, identified regulator-independent contributions, and introduced special-function parametrizations useful for analytic continuation and fast numerical solvers.

The numerical analysis complemented these findings by verifying the accuracy of the approximations, exploring the global solution space via continuation methods, and confirming the expected scaling and stability properties. In particular, the exact-versus-approximate comparison (Fig. 1) demonstrated the validity of analytic control formulas across a wide parameter range. Numerical evaluation of the effective energy functional further clarified the stability of solutions and their interpretation in terms of minima and metastability.

Physically, the nonlinear feedback embodied in the equation realizes essential mechanisms such as dynamical mass generation, dimensional transmutation, and susceptibility divergence at criticality. The robustness of these phenomena against regulator choice underlines their universality, echoing the behavior of nonperturbative quantum field theories. Moreover, the structural parallels with the NJL model, Dyson–Schwinger approaches to QCD, and finite-temperature effective potentials suggest that insights gained here can inform our understanding of complex strongly coupled systems.

Several avenues for future work emerge naturally from this study. One direction is to generalize the kernel beyond the sharp cutoff to more realistic momentum-dependent interactions, thereby moving closer to QCD-inspired gap equations. Another is to incorporate finite temperature and chemical potential, exploring whether the simplified model can reproduce qualitative features of the QCD phase diagram, such as crossovers and critical endpoints. Finally, connecting these analytic and numerical results to lattice simulations or to effective beyond-Standard-Model scenarios would provide a valuable test of the universality we have identified.

In conclusion, the nonlinear mass equation serves as a tractable yet illuminating theoretical laboratory. Its study underscores how relatively simple self-consistency conditions encode rich mathematical structures and profound physical implications. By advancing both analytic control and numerical resolution, we have laid the groundwork for applying similar strategies to more sophisticated equations at the frontiers of particle physics.

Data Availability

The manuscript has no associated data or the data will not be deposited.

Conflicts of Interest

The authors declare that there is no conflict of interest.

Ethical Considerations

The authors have diligently addressed ethical concerns, such as informed consent, plagiarism, data fabrication, misconduct, falsification, double publication, redundancy, submission, and other related matters.

Funding

This research did not receive any grant from funding agencies in the public, commercial, or nonprofit sectors.

References

[1] C. D. Roberts and A. G. Williams, Dyson–Schwinger equations and their application to hadronic physics, Prog. Part. Nucl. Phys. 33, 477–575, (1994).

[2] R. Alkofer and L. von Smekal, The infrared behaviour of QCD Green's functions: Confinement, dynamical symmetry breaking, and hadrons as relativistic bound states, Phys. Rept. 353, 281–465, (2001).

[3] Y. Nambu and G. Jona-Lasinio, Dynamical model of elementary particles based on an analogy with superconductivity. I, Phys. Rev. 122, 345 (1961).

[4] J. Bardeen, L. N. Cooper, and J. R. Schrieffer, Theory of superconductivity, Phys. Rev. 108, 1175 (1957).

[5] M. E. Peskin and D. V. Schroeder, An Introduction to Quantum Field Theory, Westview Press, 1995.

[6] J. C. Collins, Renormalization, Cambridge University Press, 1984.

[7] C. Itzykson and J.-B. Zuber, Quantum Field Theory, McGraw-Hill, 1980.

[8] R. J. Rivers, Path Integral Methods in Quantum Field Theory, Cambridge University Press, 1987.

[9] C. S. Fischer, Infrared properties of QCD from Dyson–Schwinger equations, J. Phys. G 32, R253 (2006).

[10] P. Maris and C. D. Roberts, Dyson–Schwinger equations: A tool for hadron physics, Int. J. Mod. Phys. E 12, 297–365, (2003).